

# Ellipsometric characterization of nanocrystals in porous silicon

P. Petrik<sup>\*</sup>, M. Fried, É. Vázquez, T. Lohner, E. Horváth, O. Polgár,  
P. Basa, I. Bársony, J. Gyulai

*Research Institute for Technical Physics and Materials Science, P.O. Box 49, H-1525 Budapest, Hungary*

Available online 3 July 2006

## Abstract

Porous silicon layers (PSLs) were prepared by electrochemical etching of p-type single-crystalline silicon (c-Si) wafers having different dopant concentrations to obtain systematically changing sizes of nanocrystals (walls). The microstructure of the porous material was characterized using spectroscopic ellipsometry with multi-layer effective medium approximation (EMA) models. The dielectric function of PSL is conventionally calculated using EMA mixtures of c-Si and voids. The porosity is described by the concentration of voids. Some PSL structures can be described only by adding fine-grained polycrystalline silicon (nc-Si) reference material to the EMA model. Modified model dielectric functions (MDF) of c-Si have been shown to fit composite materials containing nanocrystalline regions, either by fitting only the broadening parameter or also other parameters of the parametric oscillator in MDF. The broadening parameter correlates with the long-range order in the crystalline material, and, as a consequence, with the size of nanocrystals. EMA and MDF models were used to describe systematically changing nanostructure of PSLs. Volume fraction of nc-Si in EMA and broadening parameter in MDF provide information on the nanocrystal size. The longer-term goal of this work is to provide a method for the quantitative characterization of nanocrystal size using quick, sensitive and non-destructive optical techniques.

© 2006 Elsevier B.V. All rights reserved.

*Keywords:* Porous silicon layers; Effective medium approximation; Model dielectric functions

## 1. Introduction

Microstructure of composite materials is modelled mostly by effective medium approximation (EMA) [1,2]. Composite materials include, among others, different kinds of layers prepared by deposition (for example, polycrystalline silicon, pc-Si) or etching (porous silicon layers, PSL). Some PSL structures can be modelled by mixing single-crystalline silicon (c-Si) and voids. pc-Si can be modelled with a similar model including c-Si, voids and amorphous silicon (a-Si) [3,4]. The latter accounts for the amorphous phase remaining in the structure. It has been revealed that certain types of PSL and pc-Si structures can be better fitted using fine-grained polycrystalline silicon (nc-Si [5]) in the EMA mixture [6,7]. It was assumed that nc-Si accounts for the increased number of grain boundaries in fine-grained structures, i.e. the vanishing long-range order in the crystalline material. Adachi et al. described the same phenomenon in ion implanted Si using model dielectric function (MDF) based on critical point (CP)

calculations of c-Si [8,9]. Using MDF, decreasing long-range order is consistent with increasing broadening parameters of the CP oscillators. In the present work, we use PSL layers prepared by electrochemical etching of differently doped p-type c-Si substrate to obtain a model material of systematically changing nanocrystal (wall) sizes. The PSL layers were characterized using the EMA as well as the MDF approach.

## 2. Experimental

p-Type (1 0) Si samples with resistivities of  $R = 0.001, 0.003, 0.010, 0.030, \text{ and } 0.090 \Omega \text{ cm}$  (B concentrations ranging from  $8 \times 10^{19}$  to  $3 \times 10^{17} \text{ cm}^{-3}$ ) were etched electrochemically using an electrolyte composition of 50% hydrofluoric acid and 100% ethanol with a ratio of 1:1. The layer thicknesses were around 500 nm. The structures depending on  $R$  were measured by secondary electron microscopy (SEM).

The ellipsometric measurements were performed by a Woollam M-2000F rotating compensator ellipsometer in the wavelength range of 250–1000 nm in 481 points, at angles of incidence of 70°, 75° and 80°. Typical spectra are plotted in Fig. 1. Only every 10th measured points were plotted for the better visibility. In contrast to rotating polariser ellipsometers,

<sup>\*</sup> Corresponding author. Tel.: +36 1 3922222; fax: +36 1 3922226.

E-mail address: [petrik@mfa.kfki.hu](mailto:petrik@mfa.kfki.hu) (P. Petrik).

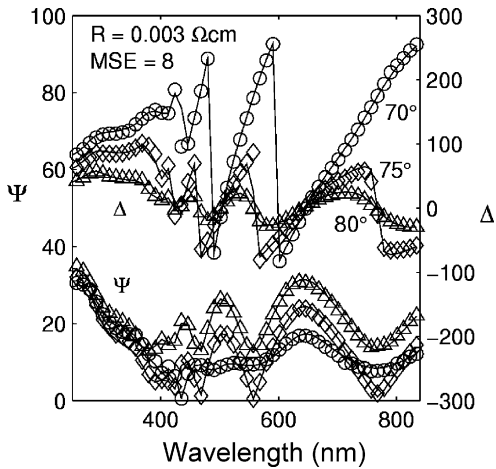


Fig. 1. Measured and fitted ellipsometric spectra for  $R = 0.003 \Omega \text{ cm}$ .

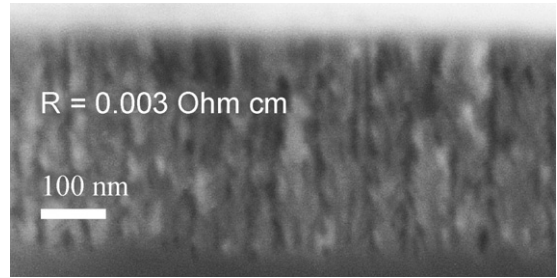


Fig. 3. SEM micrograph on a fracture of PSLs for  $R = 0.003 \Omega \text{ cm}$ .

rotating compensator ellipsometers measure  $\Delta$  directly, consequently  $\Psi$  and  $\Delta$  are plotted rather than  $\tan \Psi$  and  $\cos \Delta$ .

### 3. Discussion

Fig. 2 shows SEM micrographs on fractures of PSL altering from columnar ( $R = 0.001 \Omega \text{ cm}$ ) through dendritic ( $R = 0.003\text{--}0.010 \Omega \text{ cm}$ ) to sponge-like ( $R = 0.03\text{--}0.09 \Omega \text{ cm}$ ) structure. The wall/crystallite sizes for  $R = 0.001, 0.003$  and  $0.010 \Omega \text{ cm}$  are 15–20, 10–15 and 7–10 nm, respectively. Resolution of SEM was too low to measure crystallite sizes for  $R = 0.030$  and  $0.090 \Omega \text{ cm}$ , but based on literature data, they are assumed to decrease with increasing  $R$  down to some nanometers [10,11].

Although SEM does not show a significantly different structure at the interfaces (see Fig. 3 for  $R = 0.003 \Omega \text{ cm}$ ), the fit improves considerably when modelling the surface of the PSL and the interface to the c-Si substrate. This is assumed to be caused by the surface and interface roughness, which is consistent with previous results [5,12]. The thickness of interface layers is typically 30–50 nm on both sides of PSL.

The fitted parameters for models of improving complexity are compiled in Table 1. Dielectric function of each sub-layer is calculated using the EMA composition of c-Si, nc-Si and voids. Note the large improvement in fit quality (mean square error, MSE) when adding component nc-Si to the single-layer model (Model 12). The fit improves further when taking into account the surface layer (Model 26) and also the interface layer (Model 39, see Fig. 1 for fitted spectra). The parameters do not present a

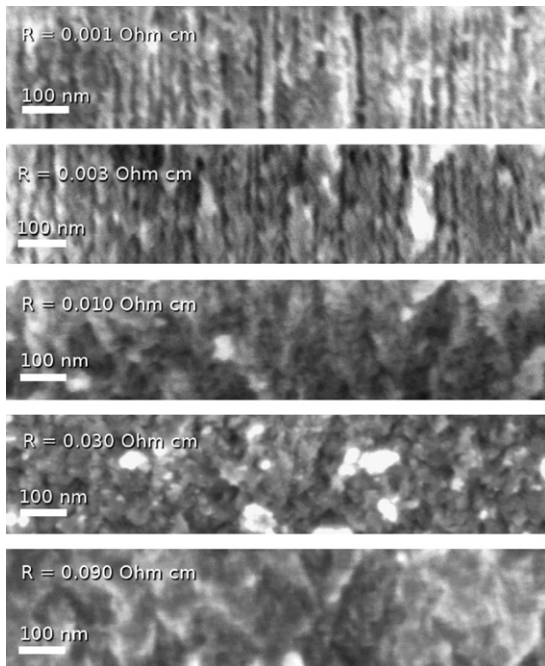


Fig. 2. SEM micrographs on fractures of PSLs.

Table 1

Optical models of increasing complexity and fitted parameters for  $R = 0.003 \Omega \text{ cm}$ . For three-layer models, Layer 1 is the interface to substrate and Layer 3 is the surface layer. First and second digits of model names denote number of layers and parameters, respectively. Parameters  $f_v$  and  $f_n$  denote the volume fractions of voids and nc-Si, respectively. Volume fraction of c-Si is  $f_c = 1 - (f_v + f_n)$ .  $d$  denotes layer thickness

Model	Substrate	Layer 1	Layer 2	Layer 3	MSE
12	c-Si	$d_1 = 338.1 \pm 0.1 \text{ nm}$ , $f_v = 0.43 \pm 0.001$			27.3
13	c-Si	$d_1 = 340.1 \pm 0.6 \text{ nm}$ , $f_v = 0.44 \pm 0.001$ , $f_n = 0.17 \pm 0.01$			16.0
26	c-Si	$d_1 = 320.8 \pm 0.9 \text{ nm}$ , $f_v = 0.46 \pm 0.001$ , $f_n = 0.18 \pm 0.004$	$d_2 = 29.6 \pm 1.0 \text{ nm}$ , $f_v = 0.44 \pm 0.001$ , $f_n = 0.34 \pm 0.01$		11.2
39	c-Si	$d_1 = 19.1 \pm 0.3 \text{ nm}$ , $f_v = 0.32 \pm 0.02$ , $f_n = 2.22 \pm 0.23$	$d_2 = 313.0 \pm 1.1 \text{ nm}$ , $f_v = 0.48 \pm 0.001$ , $f_n = 0.21 \pm 0.01$	$d_3 = 38.0 \pm 0.7 \text{ nm}$ , $f_v = 0.45 \pm 0.001$ , $f_n = 0.29 \pm 0.01$	7.6

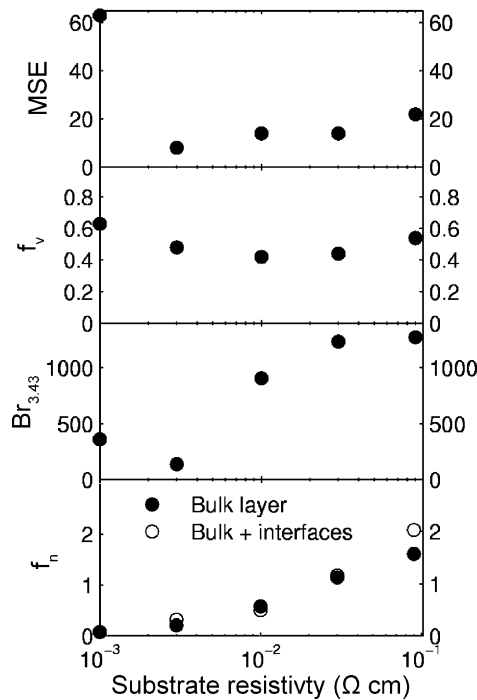


Fig. 4. Fitted volume fractions of nc-Si ( $f_n$ ) and voids ( $f_v$ ) as well as fit quality (MSE) of Model 39, together with the broadening parameter of CP at 3.43 eV ( $Br_{3,43}$ ) calculated using MDF.

strong correlation, not even in case of Model 39 with nine parameters. Fitted volume fractions of void ( $f_v$ ) are measured very sensitively without strong correlation with other parameters even for multilayer models, while correlation between fitted volume fractions of nc-Si ( $f_n$ ) are stronger but acceptable.

$f_n$ ,  $f_v$ , and MSE corresponding to Model 39 are shown in Fig. 4 as functions of  $R$ .  $f_n$  of the bulk layer increases with increasing  $R$ . The same dependence is found when calculating the integral of  $f_n$  taking into account the interfaces:  $f_{n\Sigma} = (d_1f_{n1} + d_2f_{n2} + d_3f_{n3}) / (d_1 + d_2 + d_3)$ , using the notation of Table 1, see open symbols in Fig. 4. Note that  $f_n > 1$  for  $R > 0.030 \Omega \text{ cm}$ , i.e.  $f_c < 0$  (taking into account that  $f_v \sim 0.5$ ). The physical background is shown in Fig. 5 by plotting the imaginary part of the complex dielectric function ( $\epsilon_2$ ) for  $f_v \sim 0.5$  and  $f_n = 0 \rightarrow 1$  ( $f_c = 0.5 \rightarrow [-0.5]$ ). Increasing  $f_n$  is consistent with an increase of broadening, a decrease of amplitude, and a red-shift of the absorption peaks. This tendency continues for  $f_c < 0$  as shown in the inset, which means that the measured material has smaller crystallite size than the reference material nc-Si. Note the huge effect of mixing voids. Comparing  $\epsilon_2$  of c-Si (dash-dotted line) with  $\epsilon_2$  of the EMA mixture of  $f_v = 0.5$  and  $f_n = 0 \rightarrow 1$  (solid lines), it is clear that  $\epsilon_2$  of the layer is more sensitive to mixing void with c-Si than nc-Si with c-Si due to the higher difference in  $\epsilon_2$  in case of c-Si and voids. This is the explanation of the higher sensitivity (lower confidence limits) of voids ( $f_v$ ) shown in Table 1.

Decreasing nanocrystal size (vanishing long-range order) can also be described by fitting the broadening parameter using MDF [8,9]. Fig. 4 shows the broadening parameter  $Br_{3,43}$  of the CP at 3.43 eV calculated from the three-layer model, but using MDF in spite of EMA to determine the dielectric function of PSL. The parameterized dielectric function model of c-Si was

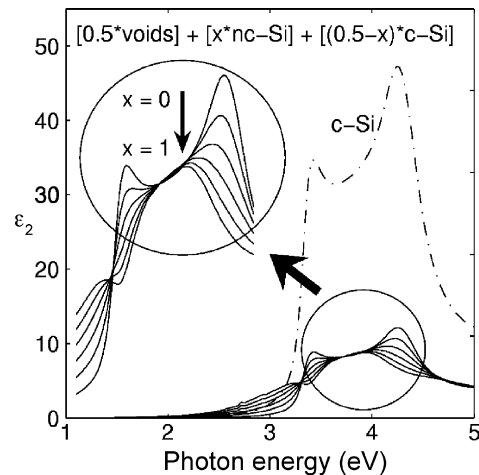


Fig. 5. Imaginary part of the dielectric function  $\epsilon_2$  for EMA compositions of  $f_v = 0.5$ ,  $f_n = x$ , and  $f_c = 0.5 - x$ , for  $x = 0 \rightarrow 1$ .  $\epsilon_2$  of c-Si is shown by dash-dotted line.

used as starting point, fitting only the broadening parameter of the transition at 3.43 eV. The measured spectrum was restricted to 1.5–3.9 eV to suppress the influence of CP at 4.2 eV. The fit quality was the same as for the EMA model.  $Br_{3,43}$  increases rapidly with increasing  $R$  showing a similar behaviour as  $f_n$ , except for the  $R = 0.001 \Omega \text{ cm}$  sample. Note that MSE of EMA (Model 39) shows also an anomalous behaviour being significantly higher for  $R = 0.001 \Omega \text{ cm}$  than for  $R \geq 0.003 \Omega \text{ cm}$ , which may be due to anisotropy caused by the columnar structure not taken into account by our model. A possible enhancement of the optical model is to take into account, at the same time, the anisotropy and the other parameters of the MDF. The good fit in cases of  $R \geq 0.003 \Omega \text{ cm}$  indicates that anisotropy can be neglected, especially compared to high sensitivity to crystallite sizes.

#### 4. Conclusions

PSLs with crystallite sizes ranging from slightly above 20 nm down to some nanometers were prepared and used as model materials to test EMA and MDF models. The crystallite size revealed strong correlation with  $f_n$  and  $Br_{3,43}$  calculated using EMA and MDF in three-layer models. The results suggest that SE can be used as a fast and non-invasive method for the quantitative measurement of crystallite size.

#### Acknowledgements

Financial support of the Hungarian Scientific Research Fund (OTKA T047011, K61725, and T043704) is acknowledged. P. P. and M. F. are grantees of the Bolyai János Scholarship.

#### References

- [1] D.E. Aspnes, Thin Solid Films 89 (1982) 249.
- [2] R.W. Collins, A.H. Clark, S. Guha, C.-Y. Huang, J. Appl. Phys. 57 (1985) 4566.

- [3] M. Modreanu, M. Gartner, C. Cobianu, B. O’Looney, F. Murphy, *Thin Solid Films* 450 (2004) 105.
- [4] M. Gartner, M. Modreanu, C. Cobianu, R. Gavrilă, M. Danila, *Sens. Actuators A* 99 (2002) 160.
- [5] G.E. Jellison Jr., M.F. Chrisholm, S.M. Gorbatkin, *Appl. Phys. Lett.* 62 (1993) 3348.
- [6] M. Fried, T. Lohner, O. Polgár, P. Petrik, É. Vázsonyi, I. Bársony, J.P. Piel, J.L. Stehle, *Thin Solid Films* 276 (1996) 223.
- [7] P. Petrik, T. Lohner, M. Fried, L.P. Biró, N.Q. Khánh, J. Gyulai, W. Lehnert, C. Schneider, H. Ryssel, *J. Appl. Phys.* 87 (2000) 1734.
- [8] S. Adachi, H. Mori, M. Takahashi, *J. Appl. Phys.* 93 (2003) 115.
- [9] K. Tsunoda, S. Adachi, M. Takahashi, *J. Appl. Phys.* 91 (2002) 2936.
- [10] V. Lehmann, U. Gösele, *Appl. Phys. Lett.* 58 (1991) 856.
- [11] A.G. Cullis, L.T. Canham, P.D.J. Calcott, *J. Appl. Phys.* 82 (1997) 909.
- [12] É. Vázsonyi, E. Szilágyi, P. Petrik, Z.E. Horváth, T. Lohner, M. Fried, G. Jaslovszky, *Thin Solid Films* 388 (2001) 295.